

## Large reversible magnetocaloric effects in ErFeSi compound under low magnetic field change around liquid hydrogen temperature

H. Zhang, B. G. Shen, Z. Y. Xu, J. Shen, F. X. Hu et al.

Citation: *Appl. Phys. Lett.* **102**, 092401 (2013); doi: 10.1063/1.4794415

View online: <http://dx.doi.org/10.1063/1.4794415>

View Table of Contents: <http://apl.aip.org/resource/1/APPLAB/v102/i9>

Published by the [American Institute of Physics](http://www.aip.org).

### Related Articles

Investigation of the critical behavior in Mn<sub>0.94</sub>Nb<sub>0.06</sub>CoGe alloy by using the field dependence of magnetic entropy change

*J. Appl. Phys.* **113**, 093902 (2013)

Positive and negative magnetocaloric effects in CeSi

*J. Appl. Phys.* **113**, 17A903 (2013)

The universal behavior of inverse magnetocaloric effect in antiferromagnetic materials

*J. Appl. Phys.* **113**, 17A902 (2013)

Influence of magnetic interactions between phases on the magnetocaloric effect of composites

*Appl. Phys. Lett.* **102**, 082402 (2013)

Magnetocaloric effect in inhomogeneous ferromagnets

*J. Appl. Phys.* **113**, 073907 (2013)

### Additional information on *Appl. Phys. Lett.*

Journal Homepage: <http://apl.aip.org/>

Journal Information: [http://apl.aip.org/about/about\\_the\\_journal](http://apl.aip.org/about/about_the_journal)

Top downloads: [http://apl.aip.org/features/most\\_downloaded](http://apl.aip.org/features/most_downloaded)

Information for Authors: <http://apl.aip.org/authors>

## ADVERTISEMENT

**AIP** | Applied Physics  
Letters

**EXPLORE WHAT'S NEW IN APL**

**SUBMIT YOUR PAPER NOW!**

**SURFACES AND INTERFACES**  
Focusing on physical, chemical, biological, structural, optical, magnetic and electrical properties of surfaces and interfaces, and more...

**ENERGY CONVERSION AND STORAGE**  
Focusing on all aspects of static and dynamic energy conversion, energy storage, photovoltaics, solar fuels, batteries, capacitors, thermoelectrics, and more...

## Large reversible magnetocaloric effects in ErFeSi compound under low magnetic field change around liquid hydrogen temperature

H. Zhang,<sup>1,a)</sup> B. G. Shen,<sup>2</sup> Z. Y. Xu,<sup>2</sup> J. Shen,<sup>3</sup> F. X. Hu,<sup>2</sup> J. R. Sun,<sup>2</sup> and Y. Long<sup>1</sup>

<sup>1</sup>*School of Materials Science and Engineering, University of Science and Technology of Beijing, Beijing 100083, People's Republic of China*

<sup>2</sup>*State Key Laboratory for Magnetism, Institute of Physics, Chinese Academy of Sciences, Beijing 100190, People's Republic of China*

<sup>3</sup>*Key laboratory of Cryogenics, Technical Institute of Physics and Chemistry, Chinese Academy of Sciences, Beijing 100190, People's Republic of China*

(Received 20 September 2012; accepted 21 February 2013; published online 4 March 2013)

Magnetic properties and magnetocaloric effects (MCEs) of ternary intermetallic ErFeSi compound have been investigated in detail. It is found that ErFeSi exhibits a second-order magnetic transition from ferromagnetic to paramagnetic states at the Curie temperature  $T_C = 22$  K, which is quite close to the liquid hydrogen temperature (20.3 K). A thermomagnetic irreversibility between zero-field-cooling and field-cooling curves is observed below  $T_C$  in low magnetic field, and it is attributed to the narrow domain wall pinning effect. For a magnetic field change of 5 T, the maximum values of magnetic entropy change ( $-\Delta S_M$ ) and adiabatic temperature change ( $\Delta T_{ad}$ ) are 23.1 J/kg K and 5.7 K, respectively. Particularly, the values of  $-\Delta S_M$  and refrigerant capacity reach as high as 14.2 J/kg K and 130 J/kg under a magnetic field change of 2 T, respectively. The large MCE without hysteresis loss for relatively low magnetic field change suggests that ErFeSi compound could be a promising material for magnetic refrigeration of hydrogen liquefaction. © 2013 American Institute of Physics. [<http://dx.doi.org/10.1063/1.4794415>]

Since the discovery of magnetocaloric effect (MCE),<sup>1</sup> magnetic refrigeration based on MCE has been proved to be an attractively alternative technology to the conventional gas compression-expansion refrigeration which possesses the key issues of low efficiency and environmental contamination.<sup>2,3</sup> In 1997, Pecharsky *et al.* reported a giant MCE of Gd<sub>5</sub>Si<sub>2</sub>Ge<sub>2</sub> near room temperature ( $T_C = 276$  K), which is caused by a first-order field induced magnetic and structural transitions.<sup>4</sup> Since then, a great deal of attention has been paid to search for magnetic refrigerants in view of domestic or industrial applications near room temperature.<sup>5–8</sup> On the other hand, the research on systems exhibiting large MCEs at low temperature is also important due to their potential utilization in the refrigeration for gas liquefaction.<sup>3,9</sup> Hydrogen is considered as one of the most possible candidates for clean energy sources because of its high energy density and friendly environment. Generally, hydrogen gas needs to be cooled down to liquid form for its storage and transportation. It has been reported that the Carnot magnetic refrigerator (CMR) achieved an efficiency of 90% in the liquefaction stage.<sup>10</sup> Therefore, it is significant to develop advanced magnetic refrigerants that show large MCEs around the liquid hydrogen temperature (20.3 K) and are suitable for applications in CMR.

Usually, the magnitude of MCE can be characterized by magnetic entropy change ( $\Delta S_M$ ) and/or adiabatic temperature change ( $\Delta T_{ad}$ ) upon the variation of magnetic field. Besides, refrigerant capacity (RC) is considered as another important parameter to quantify the heat transferred between the hot and cold sinks in an ideal refrigeration cycle. Recently, a variety of rare earth (R)-3d transition metal (TM) intermetallic

compounds have been reported to exhibit great MCEs at low temperature range because of the first-order phase transition (FOPT).<sup>11,12</sup> Unfortunately, FOPT usually accompanies with remarkable thermal and magnetic hystereses, thus always lowering the effective RC. In contrast, materials with second-order phase transition (SOPT) show reversible MCEs in response to magnetic field change, which is favorable to practical applications. In addition, the permanent magnets in present market can only provide a maximum field of  $\sim 2$  T, and this fact indicates that a large MCE under low magnetic field change is desirable for the fulfillment of a magnetic refrigerator simply using permanent magnets. Consequently, it is necessary to explore magnetic refrigerant materials that undergo a SOPT near liquid hydrogen temperature and present large MCEs especially under low magnetic field change. In present work, we report a detailed study on the magnetic properties and MCE of ErFeSi compound.

The polycrystalline ErFeSi compound was synthesized by arc-melting appropriate proportion of constituent components with the purity better than 99.9 wt. % in a water-cooled copper hearth under purified argon atmosphere. The as-cast sample was then annealed in a high-vacuum quartz tube at 1373 K for 35 days. Powder X-ray diffraction (XRD) measurement was performed at room temperature by using Cu  $K\alpha$  radiation to identify the crystal structure. The Rietveld refinement confirms that the annealed sample crystallizes in a single phase with the tetragonal CeFeSi-type structure (space group  $P4/nmm$ ). The Er and Si atoms occupy the crystallographic positions  $2c$  [0.25, 0.25,  $z$ ] ( $z_{Er} = 0.67$  and  $z_{Si} = 0.20$ ), while the Fe atoms are distributed in  $2a$  [0.75, 0.25, 0]. The lattice parameters  $a$  and  $c$  were determined to be 3.920(5) and 6.792(5) Å, respectively. These results are in a good agreement with those in previous reports.<sup>13,14</sup>

<sup>a)</sup> Author to whom correspondence should be addressed. Electronic mail: zhanghuxt@gmail.com. Tel.: +86-10-82648085. Fax: +86-10-82649485.

Magnetizations were measured as functions of temperature and magnetic field by employing a MPMS SQUID VSM magnetometer from Quantum Design Inc. The specific heat capacity and ac susceptibilities were measured by using a physical property measurement system (PPMS) from Quantum Design Inc.

Figure 1(a) shows the temperature ( $T$ ) dependences of zero-field-cooling (ZFC) and field-cooling (FC) magnetizations ( $M$ ) for ErFeSi under 0.05 T. ErFeSi experiences a ferromagnetic (FM) to paramagnetic (PM) transition around the Curie temperature  $T_C = 22$  K, defined as the minimum value of  $dM/dT$  curve, which is quite close to the liquid hydrogen temperature. Besides, another anomaly is observed around  $T_i = 7$  K in ZFC curve. However, the ac susceptibility (Fig. 1(b)) and heat capacity (Fig. 4) for ErFeSi do not show any phase transition around 7 K. The origin of this anomaly will be discussed later. The inverse dc susceptibility ( $\chi^{-1}$ ) obtained under 1 T and the Curie-Weiss fit, which is plotted in the inset of Fig. 1(a). The  $\chi^{-1}$  above  $T_C$  obeys the Curie-Weiss law with a paramagnetic Curie temperature  $\theta_P = 19.7$  K and an effective magnetic moment  $\mu_{eff} = 9.84 \mu_B$ . The value of  $\mu_{eff}$  is close to the theoretical magnetic moment ( $g\sqrt{J(J+1)} = 9.59 \mu_B$ ) of  $\text{Er}^{3+}$  free ion. This fact implies the absence of localized magnetic

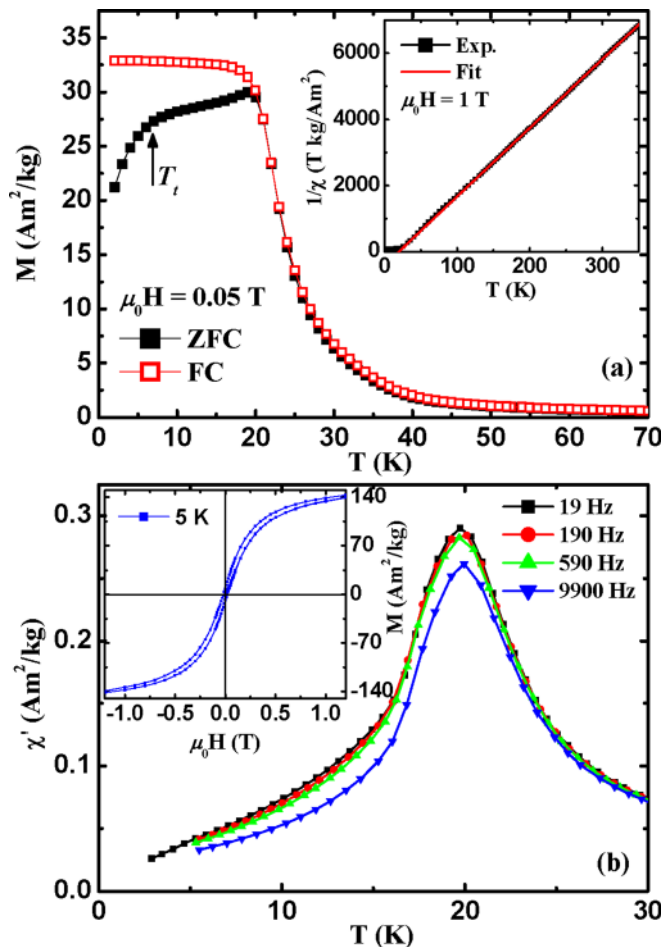


FIG. 1. (a) Temperature dependences of ZFC and FC magnetizations for ErFeSi compound under a magnetic field of 0.05 T. The inset shows the temperature variation of inverse dc susceptibility ( $\chi^{-1}$ ) fitted to the Curie-Weiss law in the field of 1 T. (b) The ac susceptibilities of ErFeSi collected at various frequencies under a zero dc field. The inset shows the magnetic hysteresis loop of ErFeSi compound at 5 K in low magnetic fields.

moment on Fe atoms in ErFeSi, which is in agreement with the result of other RFeSi compounds.<sup>14</sup>

It is clearly seen from Fig. 1(a) that the ZFC and FC curves around  $T_C$  are completely reversible as observed usually in SOPT, whereas a distinct discrepancy between ZFC and FC curves appears below  $T_C$ . This thermomagnetic irreversibility can be observed in many cases, such as spin-glass systems,<sup>15</sup> materials with competing magnetic interactions,<sup>16</sup> and ferromagnetic materials with high anisotropy.<sup>17</sup> In order to investigate the origin of this irreversibility, the ac susceptibilities  $\chi'$  of ErFeSi have been measured in various frequencies ranging from 19 to 9900 Hz and are shown in Fig. 1(b). It is found that the peak position of  $\chi'$  does not show an obvious frequency dependence, which is inconsistent with the spin-glass behavior,<sup>15</sup> suggesting that the irreversibility is not related to the spin-glass system. On the other hand, neutron diffraction investigations determined that RFeSi ( $R = \text{Nd}, \text{Tb}, \text{Dy}$ ) compounds exhibit a collinear ferromagnetic structure with magnetic moments of  $R$  ions aligned along the  $c$  axis, indicating the strong uniaxial anisotropy.<sup>14</sup> The magnetic hysteresis loop of ErFeSi at 5 K is presented in the inset of Fig. 1(b). A hysteresis with coercive field of 0.02 T is observed, further confirming the possible anisotropy of ErFeSi at low temperature. It has been reported that in materials with high anisotropy and low ordering temperature, the domain wall width could be comparable to that of lattice spacing, thus resulting in a large pinning effect.<sup>17</sup> Considering the magnetic anisotropy and low  $T_C$  for ErFeSi, the thermomagnetic irreversibility is likely attributed to the narrow domain wall pinning effect. In ZFC mode, the domain walls are pinned, and the thermal energy is not strong enough to overcome the energy barriers. This leads to the low magnetization, especially in the temperature range lower than 7 K. However, in FC mode, the magnetic field during the cooling prevents the pinning effect, and therefore the magnetization at low temperature is higher than that in ZFC mode.

The temperature dependences of ZFC and FC magnetizations under various magnetic fields are displayed in Fig. 2. With increasing magnetic field, the thermomagnetic irreversibility becomes smaller and vanishes completely when field is higher than 0.5 T. This also indicates that higher magnetic field would provide more energy for domain

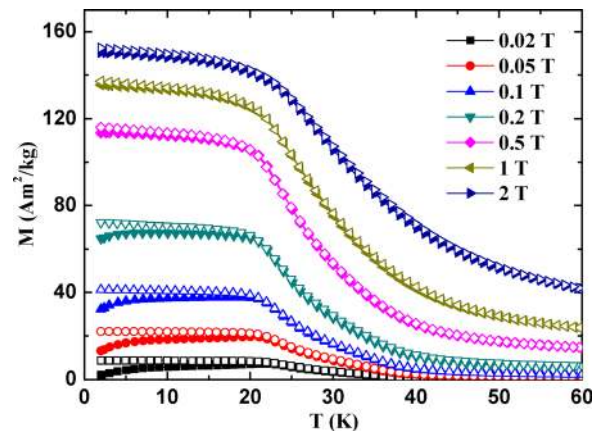


FIG. 2. Temperature dependences of the ZFC and FC magnetizations for ErFeSi under various magnetic fields.

walls to conquer the barriers of pinning effect, thus reducing the irreversibility. The magnetization isotherms of ErFeSi measured around  $T_C$  are shown in Fig. 3(a). To investigate the magnetic reversibility, the  $M$ - $H$  curves in temperature range of 19–29 K were measured in field increasing and decreasing modes. No magnetic hysteresis is found for these isotherms, which is a typical characteristic of SOPT. This perfectly reversible behavior is beneficial to the practical applications of magnetic refrigeration. In addition, it is noted that the magnetization changes largely with the variation of temperature around  $T_C$ , implying the possibility of high MCE. The saturation magnetic moment ( $\mu_S$ ) is determined to be  $7.2 \mu_B$  by extrapolating  $1/H$  to 0 using the  $M$ - $H$  curve measured at 2 K, and this value is lower than the expected  $gJ$  value of  $9.0 \mu_B$  for a free  $\text{Er}^{3+}$  ion. Similar phenomenon has also been observed in other  $R\text{FeSi}$  compounds, which is attributed to the quenching effect of a strong crystalline-electric-field (CEF).<sup>14,18</sup> The Arrott plots of ErFeSi are presented in Fig. 3(b). According to Banerjee criterion, a magnetic transition is considered as first-order when the slope of Arrott plot is negative; otherwise, it is expected to be of second-order when the slope is positive.<sup>19</sup> Neither negative slope nor inflection point is observed in the Arrott plots of ErFeSi, confirming the nature of SOPT.

Figure 4 displays the heat capacity ( $C_p$ ) curves for ErFeSi under the fields of 0, 2, and 5 T, respectively. The sharp  $\lambda$ -type peak around 21 K under zero field corresponds to the SOPT. With the increase of magnetic field, the peak gradually becomes broader and lower while it also shifts to higher temperature slightly, which is the typical characteristic of ferromagnet.<sup>9</sup> It is known that the heat capacity peak is caused by the absorption of heat which is utilized in randomization of

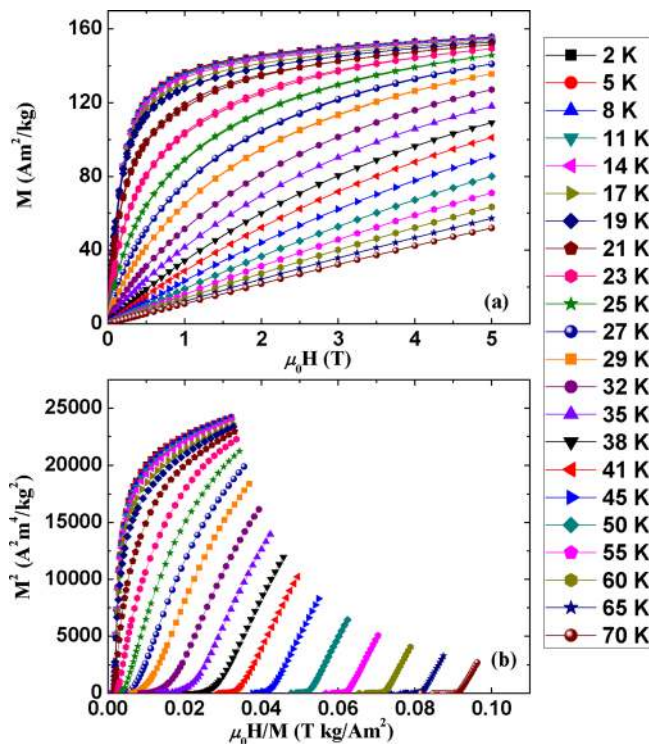


FIG. 3. (a) Magnetization isotherms and (b) Arrott plots of ErFeSi around the ordering temperature in different temperature steps.

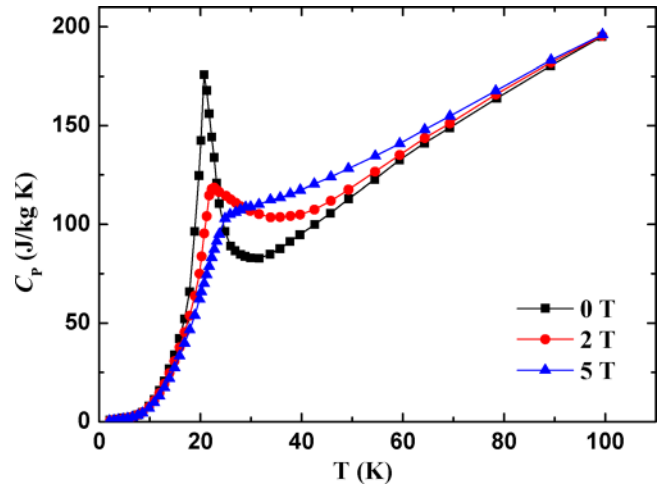


FIG. 4. Temperature dependence of heat capacity ( $C_p$ ) for ErFeSi measured in the fields of 0, 2, and 5 T, respectively.

magnetic moments around  $T_C$ . With the application of field, the randomization of moments would spread out over a wide temperature region, and the maximum peak moves towards higher temperature.<sup>4,20</sup>

As is well known, the  $\Delta S_M$  values can be calculated either from the magnetization isotherms by using the Maxwell relation  $\Delta S_M(T, H) = \int_0^H (\partial M / \partial T)_H dH$  or from the heat capacity by using the equation  $\Delta S_M(T) = \int_0^T [C_H(T) - C_0(T)] / T dT$ ,<sup>21</sup> respectively. However, sometimes the values of  $\Delta S_M$  calculated from heat capacity may be much lower than those obtained from magnetization isotherms, which is likely due to the poor contact between sample and measuring platform. For comparison, the  $\Delta S_M$  values were determined from both methods as shown in Fig. 5(a), and it is clearly seen that the  $\Delta S_M$  curves obtained from two methods match well with each other. The maximum values of  $-\Delta S_M$  reach 14.2 and 23.1 J/kg K for the field changes of 2 and 5 T, respectively. In addition, the RC was estimated by using the approach  $RC = \int_{T_1}^{T_2} |\Delta S_M| dT$ , where  $T_1$  and  $T_2$  are the temperatures corresponding to the both sides of half maximum value of  $\Delta S_M$  peak.<sup>22</sup> Thus, the RC values are obtained to be 130 and 365 J/kg for the field changes of 2 and 5 T, respectively. As mentioned before, the magnetic field of 2 T can be provided by a permanent magnet. Therefore, this large MCE of ErFeSi under low field change is favorable to practical applications. Unlike other magnetic materials with FOPT,<sup>4,11</sup> in which the large MCEs are caused by coupled magnetic and structural transitions, such giant MCE in ErFeSi is considered to be contributed mainly by the large change of magnetization during the SOPT.

As another important parameter to evaluate the MCE of magnetocaloric materials, the  $\Delta T_{ad}$  was calculated from the  $C_p$  vs.  $T$  curves by using the equation  $\Delta T_{ad}(\Delta H, T) = [T(S)_H - T(S)_0]_S$ .<sup>21</sup> Figure 5(b) shows the temperature dependence of  $\Delta T_{ad}$  of ErFeSi and the maximum values of  $\Delta T_{ad}$  are 2.9 and 5.7 K for the field changes of 2 and 5 T, respectively. For comparison, the magnetocaloric properties of ErFeSi and some other refrigerant materials with a magnetic ordering temperature around 20.3 K are listed in Table I. It can be seen that the MCE of ErFeSi, especially under the low magnetic field change, is comparable with or even larger than

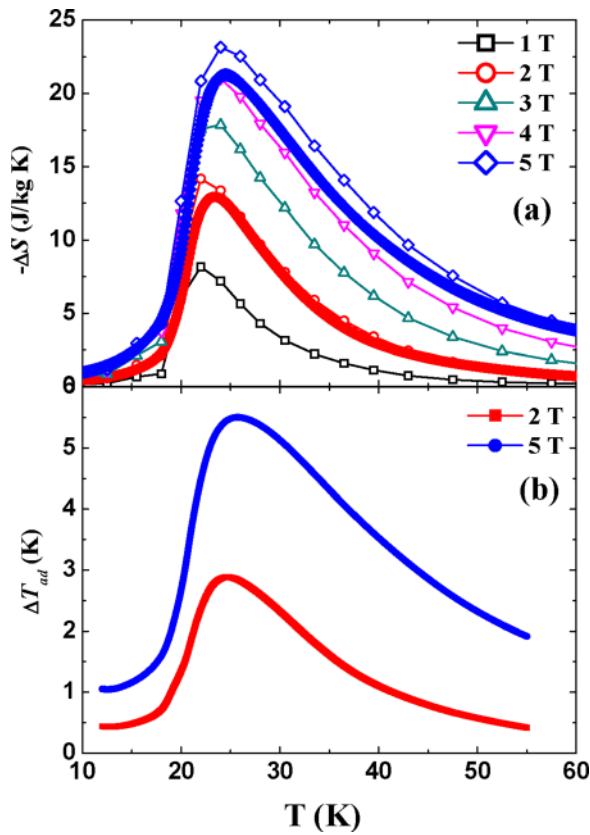


FIG. 5. (a) Magnetic entropy changes of ErFeSi calculated from magnetizations (open symbols) and heat capacity measurements (full symbols) as a function of temperature for different magnetic field changes up to 5 T. (b) Adiabatic temperature changes of ErFeSi as a function of temperature for the field changes of 2 and 5 T, respectively.

TABLE I. The ordering temperature ( $T_{ord}$ ), the magnetic entropy change  $\Delta S_M$ , adiabatic temperature change  $\Delta T_{ad}$ , and the refrigerant capacity  $RC$  for ErFeSi and some other refrigerant materials with a magnetic ordering temperature around liquid hydrogen temperature (20.3 K).

Materials	$T_{ord}$ (K)	$-\Delta S_M$ (J/kg K)		$\Delta T_{ad}$ (K)		$RC$ (J/kg)	References
		2T	5T	2T	5T		
PrNi	20	2.4	6.1	0.8	1.7	43 <sup>a</sup>	23
NdCo <sub>2</sub> B <sub>2</sub>	27	4.5	7.1	3.3	5.8 <sup>b</sup>	80 <sup>a</sup>	24
GdPd <sub>2</sub> Si	17	4.5	15	3.2	8.6	240 <sup>a</sup>	25
TbCo <sub>3</sub> B <sub>2</sub>	28	4.9	8.7	4.0 <sup>b</sup>	7.3 <sup>b</sup>	175 <sup>a</sup>	26
DyNi <sub>2</sub>	20	10.7	21.3	4.2	8.4	349 <sup>a</sup>	27
Er <sub>3</sub> Ni <sub>2</sub>	17	11.0	19.5	3.3 <sup>b</sup>	5.9 <sup>b</sup>	407 <sup>a</sup>	28
ErFeSi	22	14.2	23.1	2.9/3.4 <sup>b</sup>	5.7/7.1 <sup>b</sup>	365	This work

<sup>a</sup>The  $RC$  values are estimated from the temperature dependences of  $\Delta S_M$  in the reference literatures.

<sup>b</sup>The  $\Delta T_{ad}$  values are calculated by using the equation  $\Delta T_{ad} = -\Delta S(T, H) \times T / C_P(T, H_0)$ , where  $C_P(T, H_0)$  is zero-field heat capacity.

those of other magnetocaloric materials around the liquid hydrogen temperature.

In conclusion, ErFeSi undergoes a SOPT from FM to PM states around  $T_C = 22$  K. The thermomagnetic irreversibility between ZFC and FC curves is detected below  $T_C$  in low magnetic field due to the narrow domain wall pinning effect. The maximum values of  $-\Delta S_M$  and  $RC$  are found to

be 23.1 J/kg K and 365 J/kg for a magnetic field change of 5 T. Especially, ErFeSi exhibits a large reversible MCE under a relatively low magnetic field change (i.e., 2 T), which is comparable with or much higher than those of some magnetocaloric materials in similar temperature range. The excellent magnetocaloric performance in low magnetic field makes ErFeSi attractive candidate for magnetic refrigerant materials around liquid hydrogen temperature.

This work was supported by the National Natural Science Foundation of China (Grant No. 51001114), the National Basic Research Program of China, the Knowledge Innovation Project of the Chinese Academy of Sciences, the Hi-Tech Research and Development program of China (Grant No. 2011AA03A404).

<sup>1</sup>E. Warburg, *Ann. Phys.* **249**, 141 (1881).

<sup>2</sup>C. B. Zimm, A. Jastrab, A. Sternberg, V. K. Pecharsky, K. A. Gschneidner, Jr., M. Osborne, and I. Anderson, *Adv. Cryog. Eng.* **43**, 1759 (1998).

<sup>3</sup>K. A. Gschneidner, Jr., V. K. Pecharsky, and A. O. Tsokol, *Rep. Prog. Phys.* **68**, 1479 (2005).

<sup>4</sup>V. K. Pecharsky and K. A. Gschneidner, Jr., *Phys. Rev. Lett.* **78**, 4494 (1997).

<sup>5</sup>F. X. Hu, B. G. Shen, J. R. Sun, Z. H. Cheng, G. H. Rao, and X. X. Zhang, *Appl. Phys. Lett.* **78**, 3675 (2001).

<sup>6</sup>H. Wada and Y. Tanabe, *Appl. Phys. Lett.* **79**, 3302 (2001).

<sup>7</sup>F. X. Hu, B. G. Shen, J. R. Sun, and G. H. Wu, *Phys. Rev. B* **64**, 132412 (2001).

<sup>8</sup>H. Zhang, B. G. Shen, Z. Y. Xu, X. Q. Zheng, J. Shen, F. X. Hu, J. R. Sun, and Y. Long, *J. Appl. Phys.* **111**, 07A909 (2012).

<sup>9</sup>A. M. Tishin and Y. I. Spichkin, in *The Magnetocaloric Effect and its Applications*, edited by J. M. D. Coey, D. R. Tilley, and D. R. Vij (Institute of Physics Publishing, Bristol, 2003).

<sup>10</sup>K. Matsumoto, T. Kondo, S. Yoshioka, K. Kamiya, and T. Numazawa, *J. Phys.: Conf. Ser.* **150**, 012028 (2009).

<sup>11</sup>H. Wada, Y. Tanabe, M. Shiga, H. Sugawara, and H. Sato, *J. Alloys Compd.* **316**, 245 (2001).

<sup>12</sup>L. W. Li, K. Nishimura, and H. Yamane, *Appl. Phys. Lett.* **94**, 102509 (2009).

<sup>13</sup>O. I. Bodak, E. I. Gladyshevskii, and P. I. Kripyakevich, *Zh. Strukt. Khim.* **11**, 283 (1970).

<sup>14</sup>R. Welter, G. Venturini, and B. Malaman, *J. Alloys Compd.* **189**, 49 (1992).

<sup>15</sup>F. Yuan, J. Du, and B. L. Shen, *Appl. Phys. Lett.* **101**, 032405 (2012).

<sup>16</sup>N. K. Singh, P. Kumar, K. G. Suresh, and A. K. Nigam, *J. Appl. Phys.* **105**, 023901 (2009).

<sup>17</sup>J. L. Wang, C. Marquina, M. R. Ibarra, and G. H. Wu, *Phys. Rev. B* **73**, 094436 (2006).

<sup>18</sup>A. Prasad, C. Geibel, and Z. Hossain, *J. Magn. Magn. Mater.* **322**, 2545 (2010).

<sup>19</sup>B. K. Banerjee, *Phys. Lett.* **12**, 16 (1964).

<sup>20</sup>N. K. Singh, K. G. Suresh, A. K. Nigam, and S. K. Malik, *J. Appl. Phys.* **97**, 10A301 (2005).

<sup>21</sup>V. K. Pecharsky and K. A. Gschneidner, Jr., *J. Appl. Phys.* **86**, 565 (1999).

<sup>22</sup>K. A. Gschneidner, Jr., V. K. Pecharsky, A. O. Pecharsky, and C. B. Zimm, *Mater. Sci. Forum* **315–317**, 69 (1999).

<sup>23</sup>A. O. Pecharsky, Yu. Mozharivskiy, K. W. Dennis, K. A. Gschneidner, Jr., R. W. McCallum, G. J. Miller, and V. K. Pecharsky, *Phys. Rev. B* **68**, 134452 (2003).

<sup>24</sup>L. W. Li and K. Nishimura, *J. Phys. D: Appl. Phys.* **42**, 145003 (2009).

<sup>25</sup>R. Rawat and I. Das, *J. Phys.: Condens. Matter* **13**, L57 (2001).

<sup>26</sup>L. W. Li, D. X. Huo, H. Igawa, and K. Nishimura, *J. Alloys Compd.* **509**, 1796 (2011).

<sup>27</sup>P. J. von Ranke, V. K. Pecharsky, and K. A. Gschneidner, Jr., *Phys. Rev. B* **58**, 12110 (1998).

<sup>28</sup>Q. Y. Dong, J. Chen, J. Shen, J. R. Sun, and B. G. Shen, *Appl. Phys. Lett.* **99**, 132504 (2011).